Electronic Supplementary Information

Uncovering ZnS growth behavior and morphology control for high-performance aqueous Zn–S batteries

Sibo Wang[a], Wanlong Wu[b,*], Quanwei Jiang[a], Chen Li[a], Hua-Yu Shi[a], Xiao-Xia Liu[a,c,d] and Xiaoqi Sun[a,c,*]

[a.] Department of Chemistry, Northeastern University, Shenyang 110819, China.

[b.] College of Chemistry & Chemical Engineering, Yan'an University, Yanan 716000, China.

[c.] National Frontiers Science Center for Industrial Intelligence and Systems Optimization, Northeastern University, 3-11 Wenhua Road, Shenyang, 110819, China

[d.] Key Laboratory of Data Analytics and Optimization for Smart Industry (Northeastern University), Ministry of Education, 110819, China

*Corresponding authors. E-mail: wanlongwu@yau.edu.cn; sunxiaoqi@mail.neu.edu.cn

1 Experimental Section

1.1 Materials

Graphite foil was purchased from the SGL group (Germany). Sulfur and zinc foil were purchased from Sinopharm Chemical Reagent Co. Ltd. Ketjen black (KB) was purchased from Lion Specialty Chemicals (Japan). Carbon nanofibers (CNF) was purchased from Xianfeng Ltd. Nafion (117) was purchased from Chemours Ltd. The other reagents were obtained from Aladdin Chemical Reagent Co. Ltd.

1.2 Characterizations

The morphologies were characterized by a scanning electron microscope (HITACHI, SU8010, Japan) and a transmission electron microscope (FEI Talos F200X G2). Raman spectroscopy was conducted on BWS465-532S (B&W Tek Inc.) with a 532 nm excitation laser. The sulfide solubilities were measured by an Agilent 5110 inductively coupled plasma mass spectrometer. The sulfur concentrations in $Zn(TFSI)_2$ or $Zn(OTf)_2$ solutions were also measured and deducted from the overall concentrations after dissolving ZnS. X-ray photoelectron spectroscopy (XPS) was measured on KRATOS, Axis Ultra DLD (UK) with Al-Kα radiation as the excitation source. The date was analyzed using the CasaXPS software and calibrated by referencing the C 1s peak to 284.6 eV. X-ray diffraction (XRD) was carried out on a PANalytical Empyrean diffractometer with Cu Kα radiation. Thermogravimetric analysis (TGA) was carried out on Ruigaku TG/DTA8122 (Japan) with a heating rate of 10 ℃ min^{-1} in air atmosphere.

1.3 Electrochemical measurements

The S/KB cathodes were prepared by mixing sulfur and KB at a 5:4 weight ratio and heated at 155 ℃ for 10 hours. It was then mixed with sodium alginate binder with a weight ratio of 9:1 in water to form slurry (5:4:1 ratio of S:KB:binder). Similar procedure was applied for S/CNF cathodes, except for the S:CNF:binder weight ratio of 3:6:1 to achieve comparable electrochemical activity. The slurry was cast onto graphite foil substrate and dried at room temperature overnight. The mass loading of sulfur was around 1.8 mg cm^{-2} for regular tests or 5 mg cm^{-2} for high sulfur loading tests. The thickness/mass of Zn anode was 0.13 mm/110 mg for excess anode tests, and 0.02 mm/12 mg for N/P = 1.2 tests. Two electrode Swagelok® type cells were assembled with sulfur cathode and Zn anode. The amount of electrolyte was 100 µL. Electrochemical impedance spectroscopy (EIS) measurements were carried out in T-shaped three-electrode PFA Swagelok® type cells with S/CNF working electrode, Zn counter electrode and SCE reference electrode. The electrochemical measurements were carried out on Bio-Logic-VMP3 or LANHD-CT2001A electrochemical systems.

1.4 Computational details

Molecular dynamic (MD) simulations were performed by the Forcite module in the Materials Studio software. The model was constructed with 556 H_2O and 10 $ZnBr_2$/$Zn(OTf)_2$/$Zn(TFSI)_2$ to represent the three solutions, respectively. Geometry optimizations were firstly carried out in the Forcite module based on the convergence of the total energy (0.0001 kcal mol^{-1}) with the force of 0.005 kcal mol^{-1} $Å^{-1}$. MD simulations were then conducted by NVT and NPT ensembles at 298 K. The cutoff distances for van der Waals and electrostatic interactions were both 15.5 Å. All

simulations were carried out in the standard periodic boundary condition and the simulation time was long enough to ensure the equilibrium states of electrolyte systems. The adsorption energies of Zn-S on the surface of the (220) and (111) planes of ZnS as well as carbon tube were calculated by the CASTEP program package in Materials Studio. The exchange and correlation terms were determined using the Generalized Gradient Approximation (GGA) in the form proposed by Perdew, Burke, and Ernzerhof (PBE). The energy convergence criterion was set to 10^{-6} Hartree. In the Z direction, there was about 15 Å vacuum for erasing the effect of periodic condition for slab model.

2 Supplementary Figures and Table

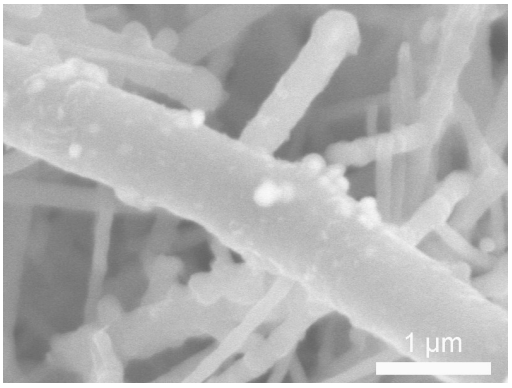

Figure S1. SEM image of pristine S/CNF electrode. The S component is attached to the surface of CNF during the melt-diffusion preparation process.

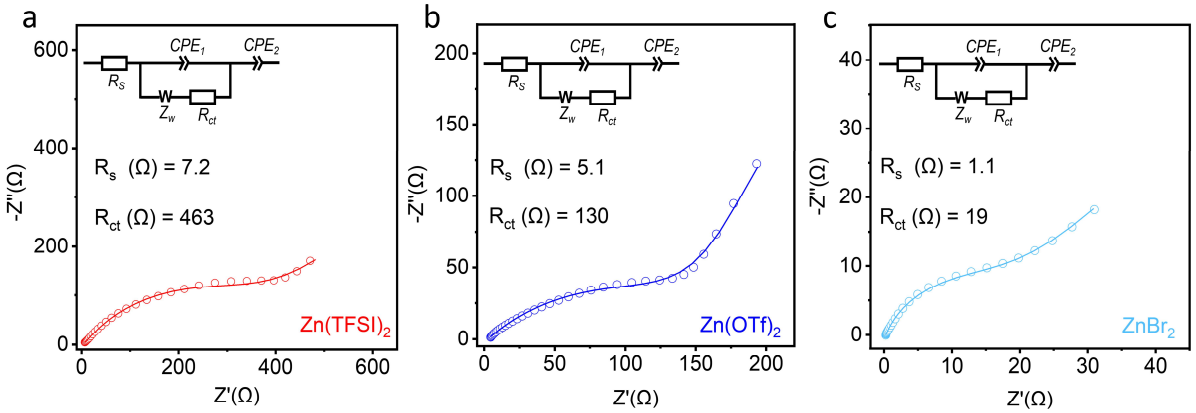

Figure S2. Nyquist plots and fitted curves of the cathodes at the half-discharged state in a) $Zn(TFSI)_2$, b) $Zn(OTf)_2$, c) $ZnBr_2$.

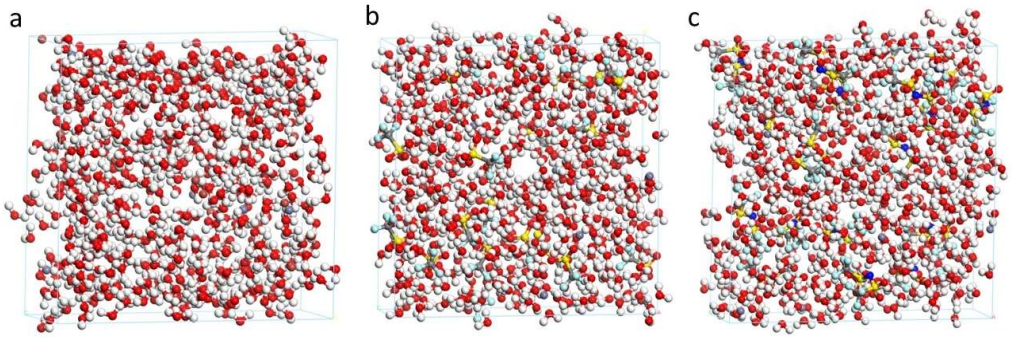

Figure S3. MD simulation snapshots of the three electrolytes of (a) $ZnBr_2$, (b) $Zn(OTf)_2$, and (c) $Zn(TFSI)_2$.

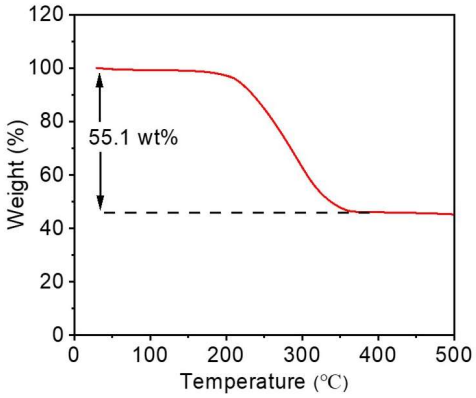

Figure S4. TGA curve of the S/KB cathode.

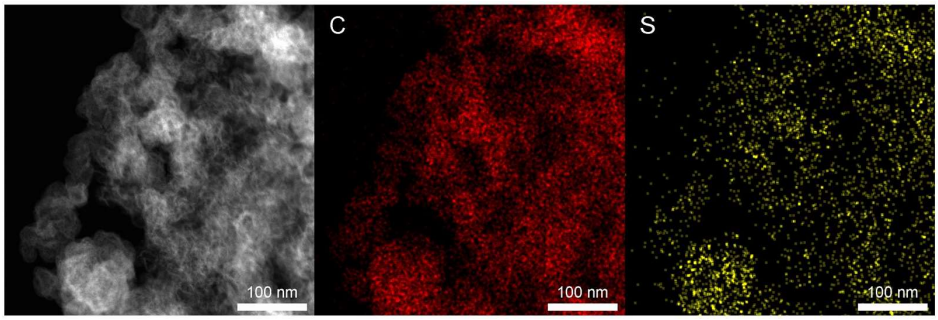

Figure S5. TEM image and EDS mappings of the S/KB cathode.

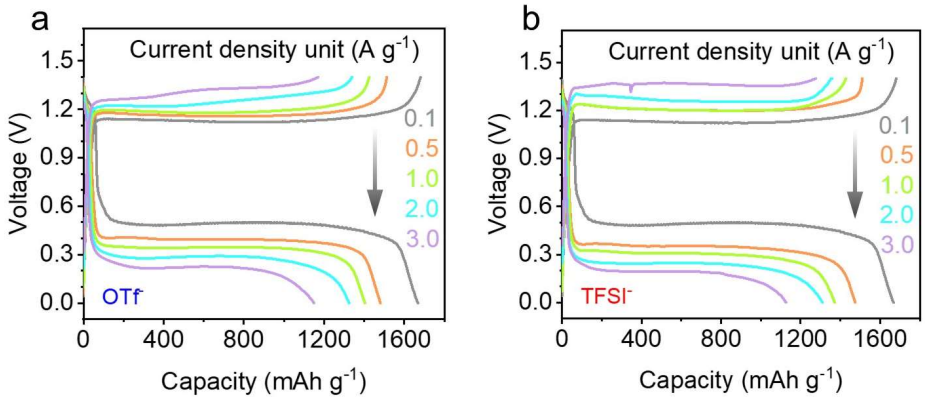

Figure S6. Charge-discharge curves of Zn-S cells in the electrolytes containing (a) OTf^- and (b) $TFSI^-$ anions at different current densities.

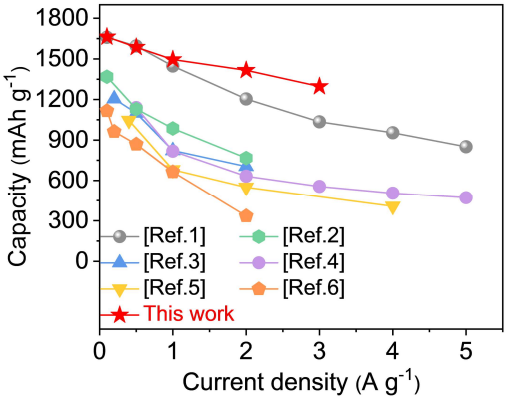

Figure S7. Electrochemical performance comparison of Zn-S batteries.

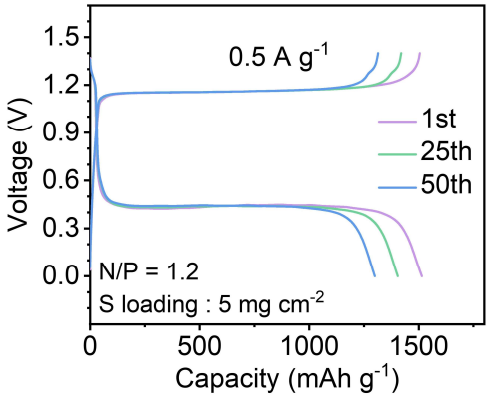

Figure S8. Charge/discharge curves of Zn-S cells in the Br^- electrolyte at different cycles at 0.5 A g^{-1} with sulfur loading of 5 mg cm^{-2} and N/P ratio of 1.2.

Table S1. The ionic conductivities and pH values of the three electrolytes.

electrolyte	ionic conductivity	pH value
$Zn(TFSI)_2$	41.3 mS cm^{-1}	4.95
$Zn(OTf)_2$	63.7 mS cm^{-1}	4.70
$ZnBr_2$	106.4 mS cm^{-1}	4.26

3 References

1. W. Wu, S. Wang, L. Lin, H. Shi, X. Sun, Energy Environ. Sci., 2023, **16**, 4326-4333.

2. Y. Guo, R. Chua, Y. Chen, Y. Cai, E. J. J. Tang, J. J. N. Lim, T. H. Tran, V. Verma, M. W. Wong, M. Srinivasan, 2023, **19** 2207133.

3. H. Zhang, Z. Shang, G. Luo. S, Jiao. R. Cao, Q. Chen, K. Lu, ACS Nano, 2021, **16**, 7344-7351

4. M. Yang, Z. Yan, J. Xiao, W. Xin, L. Zhang, H. Peng, Y. Geng, J. Li, Y. Wang, L. Liu, Z. Zhu, Angew. Chem. Int. Ed., 2022, **61**, e202212666.

5. W. Li, K. Wang, K. Jiang, Adv. Sci., 2020, **7**, 2000761.

6. T. Zhou, H. Wan, M. Liu, Q. Wu, Z. Fan, Y. Zhu, Mater. Today Energy, 2022, **27**, 101025.